ORFEUS-SPAS II EUV Spectroscopy
of ϵ CMa (B2 II)

D.H. Cohen, M. Hurwitz,
J.P. Cassinelli, S. Bowyer

March 1998

UWFDM-1067

FUSION TECHNOLOGY INSTITUTE

UNIVERSITY OF WISCONSIN

MADISON WISCONSIN

ORFEUS-SPAS II EUV Spectroscopy of ϵ CMa (B2 II)[1]

David H. Cohen

Fusion Technology Institute and Department of Astronomy,
University of Wisconsin–Madison, 1500 Engineering Drive, Madison, WI 53706
e-mail: cohen@duff.astro.wisc.edu

Mark Hurwitz

Space Sciences Laboratory, University of California, Berkeley, CA 94720
e-mail: markh@ssl.berkeley.edu

Joseph P. Cassinelli

Department of Astronomy, University of Wisconsin–Madison,
475 Charter St., Madison, WI 53706
e-mail: cassinelli@madraf.astro.wisc.edu

Stuart Bowyer

Space Sciences Laboratory, University of California, Berkeley, CA 94720
e-mail: bowyer@ssl.berkeley.edu

ABSTRACT

We report on EUV spectroscopic observations of the B bright giant ϵ CMa made during the *ORFEUS-SPAS II* mission. We assess the performance of the instrument in the EUV and find that the effective area is roughly three times that of the *EUVE* long wavelength spectrometer and that the spectral resolution is $\lambda/\Delta\lambda \approx 1250$. We identify most of the features, qualitatively compare different models, and examine the wind-broadened O V and Si IV lines, which display blue edge velocities up to 800 km s^{-1}.

Subject headings: line: identification — stars: atmospheres — stars: early-type — stars: individual (ϵ CMa) — ultraviolet: stars

---

[1]Based on the development and utilization of ORFEUS (Orbiting and Retrievable Far and Extreme Ultraviolet Spectrometers), a collaboration of the Institute for Astronomy and Astrophysics at the University of Tübingen, the Space Astrophysics Group of the University of California at Berkeley, and the Landessternwarte Heidelberg.

1.   Introduction

One of the surprising discoveries of the *EUVE* telescope was that the B star ϵ CMa (B2 II) is the brightest extrasolar source of radiation between 504 Å and 760 Å (Vallerga, Vedder, & Welsh 1993). This star is one of only two early-type stars for which high quality EUV spectra can be obtained. As such, it provides a rare opportunity to study the photosphere of a hot star below the Lyman edge, where the continuum is formed very high in the atmosphere and where wind effects and non-LTE effects are expected to be more severe than in the UV or optical. In this paper, we report on *ORFEUS-SPAS II* EUV observations of ϵ CMa between 520 Å and 665 Å, made with unprecedented spectral resolution. We describe the performance of the *ORFEUS-SPAS II* Berkeley spectrometer in the EUV, and show that the wealth of data provided in the spectrum can be used to test wind models as well as photospheric models of this early B star.

The very high EUV flux of ϵ CMa is partially due to the extremely small interstellar H I column density on the sight-line to this star ($N_H < 10^{18}$ cm^{-1}), but it is primarily caused by the unexpectedly large intrinsic Lyman continuum flux. In fact, the flux levels observed by *EUVE* are 30 times higher than the appropriate LTE Kurucz (1992) model atmosphere, and 100 times higher than a non-LTE, line-blanketed TLUSTY (Hubeny & Lanz 1992) model (Cassinelli et al. 1995). A similar, but not as extreme, excess is also seen in the *EUVE* observation of the B1 II-III star β CMa. Both stars have mid-IR excesses in addition to EUV excesses. The IR continuum between 10 μm and 15 μm in these B stars is formed in the same physical layers as the Lyman continuum between 500 Å and 700 Å. The IR continuum is dominated by free-free, which is a strictly thermal process, and a local temperature excess of about 2000 K over the Kurucz model fits both the Lyman and mid-IR continua (Cassinelli et al. 1995).

Different explanations of this purported temperature excess have been put forward since the discovery of the large EUV fluxes in ϵ CMa and β CMa. These include additional line-blanketing and non-planar effects (Aufdenberg et al. 1998), mechanical heating (Cassinelli 1996), and X-ray irradiation from the stellar wind (Cohen et al. 1996). An explanation for the EUV excess that does not assume a temperature excess has also been proposed. It relies on non-LTE effects caused by Doppler shifts in the subsonic regions of the outer atmosphere (Najarro et al. 1996). Regardless of the mechanism, reproducing the line-blanketed EUV spectrum would be an important constraint on any model.

The nature of the winds of early B stars is largely unknown because of the small number of wind-broadened lines visible in the optical and UV. Furthermore, without information about the ionization structure, the interpretation of the limited number of wind lines seen in the UV is ambiguous. With the additional constraints imposed by the measurement of

EUV wind lines in ϵ CMa it should be possible to determine the wind ionization balance and mass-loss rate of this early B star.

The *EUVE* spectroscopy, with an average resolution of $\lambda/\Delta\lambda \approx 300$, suffered from significant line-blending, making the measurement of individual line strengths impossible. Additionally, due to the extreme line-blanketing, it was not clear that the continuum level was actually reached at any point between 504 Å and the end of the *EUVE* sensitivity at 760 Å. With the new *ORFEUS-SPAS II* observations, we can resolve single features in the *EUVE* data into several individual features. These higher resolution data will be very valuable for putting tight constraints on wind models as well as testing new atmosphere models.

2. Data

The data discussed in this letter were collected with the Berkeley spectrograph aboard the *ORFEUS-SPAS II* mission flown in November/December 1996. ϵ CMa was observed five times, providing a useful integration time of 9447 s. The instrument is described in Hurwitz & Bowyer (1986, 1996) and the performance of the *ORFEUS-SPAS II* mission is described in Hurwitz et al. (1997). To attenuate scattered far ultraviolet light which would otherwise contaminate the EUV spectrum, ϵ CMa was observed through the tin-filtered aperture in diaphragm position 3. This aperture is $120''$ in diameter, displaced off axis by $5'.0$, and covered by a tin filter approximately 1500 Å thick. Extraction of the spectra and subtraction of background generally followed the procedure discussed in Hurwitz et al. (1997).

Characterization of the instrument performance in the extreme ultraviolet is more difficult than in the far ultraviolet. The only detectable diffuse emission feature is He I 584.33 Å. We used about one dozen relatively unblended features to define the overall wavelength scale for these observations. Residual errors in the wavelength solution are below 0.5 Å. For the current analysis it is not important to establish an absolute flux level, and we have not attempted to do so in any detail here, although it is expected that for filtered observations, the Berkeley spectrograph effective area is about 3 times that of the *EUVE* spectrograph at wavelengths of overlap. The peak transmission of the filter is only $\sim 20\%$; for white dwarfs and other sources that do not require the filter, the effective area greatly exceeds that of *EUVE*.

3. Discussion

In order to identify lines, we compared the data to a TLUSTY $T_{\rm eff} = 21000$ K, $\log g = 3.2$ non-LTE synthetic spectrum that uses the Kurucz line-list (see Cassinelli et al. 1995), as well as to several hotter models ($T_{\rm eff} = 23000$ K and $T_{\rm eff} = 24700$ K). The same lines are generally present in these different models, although N II and C II are much stronger in the nominal, 21000 K, model and the balance between Fe IV and Fe III varies among the models. We checked our identifications against the line-list of Verner (1996). Overall, there is very good agreement between these two references. As can be seen in Figure 1, many strong lines and numerous weak ones were identified, with very few features left unidentified.

Despite the relatively high resolution of the data, the spectrum still suffers from line-blending due to the very high density of features. It is not clear if the continuum level is actually reached anywhere in the *ORFEUS-SPAS II* spectrum, although it may be near 528 Å, and possibly a few other places. It should be noted that ϵ CMa has a very low projected rotational velocity of 35 km s^{-1} (Uesugi & Fukuda 1982), so that narrow photospheric lines are not resolved. The strongest unambiguously identified features – from C II, N II, O II, and He I – are all predicted to be among the strongest lines in the non-LTE 21000 K model. However, iron seems to be more highly ionized (predominantly Fe IV rather than Fe III) than in the 21000 K model, although the iron features are often heavily blended and thus are difficult to identify individually. The 21000 K model makes relatively accurate predictions of the absorption features even as it fails to match the continuum level by nearly two orders of magnitude. However, detailed modeling in which individual line strengths are compared to the data will be necessary before the validity of specific model characteristics can be evaluated. Fortunately, with the higher resolution available with the *ORFEUS-SPAS II* data, these quantitative comparisons can now be made.

To assess the resolution achieved in this data, we examined several intrinsically narrow, relatively unblended lines and measured their FWHM's. The cleanest example of such a well-behaved feature is the Si III line at 566 Å, shown in Figure 2. Its FWHM is roughly 240 km s^{-1}, implying a resolution of $\lambda/\Delta\lambda \approx 1250$. Other lines, such as the He I line at 584 Å, give similar results. This resolution is less than that achieved in the far ultraviolet.

There are several possible explanations for the poorer than expected resolution. The off-axis position of the filtered aperture introduces optical aberrations, but numerical raytraces indicate that these can contribute only to a modest decline in the system resolution (from an ideal of $\lambda/\Delta\lambda \approx 5000$ for on-axis spectra to about $\lambda/\Delta\lambda \approx 4000$ for these off-axis pointings). Simple Z-axis defocus did not appear to be significant in the FUV (see Hurwitz et al. 1997), but these EUV spectra are dispersed by diffraction grating B, an
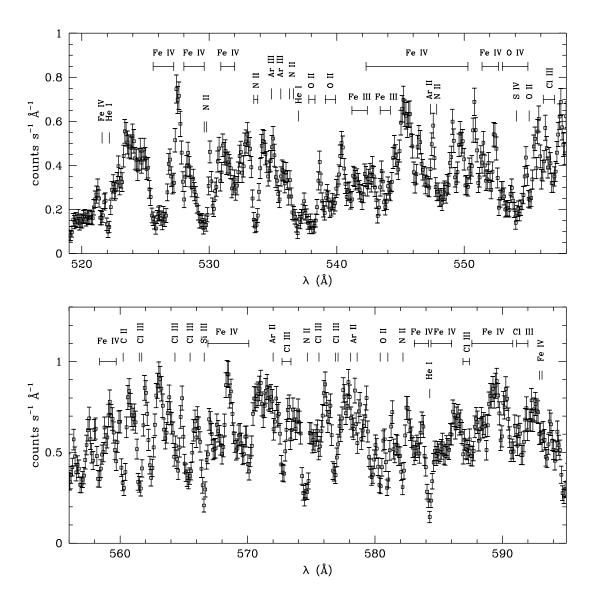
Fig. 1.— Coadded *ORFEUS-SPAS II* spectrum from data collected over five orbits, with bin sizes of 0.103 Å and 1 σ statistical uncertainties indicated. Strong lines are identified above the spectra. Note that the wavelength scale is accurate to about 0.5 Å.
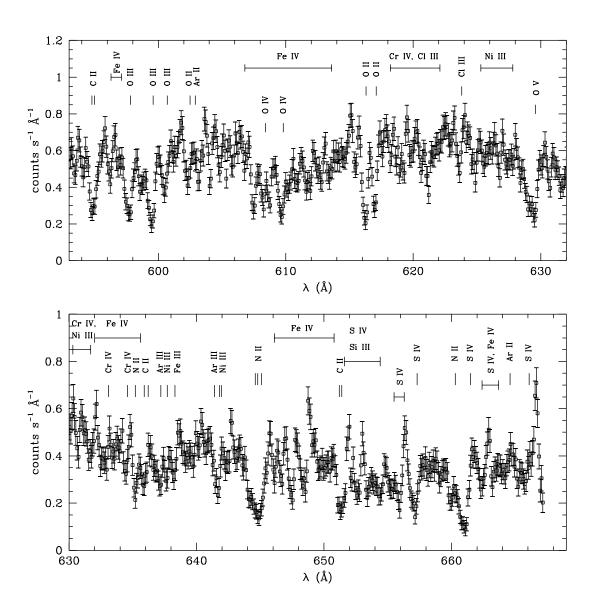
Fig. 1.— continued

independent optic. This opens the possibility that Z-axis defocus may have been present. However, all four gratings were brought to a common focus during laboratory calibration, and the Z-axis positions of the grating holders are monitored electronically. No significant Z-axis motions occurred between the laboratory calibration and in-flight operations. We note, however, that the grating B spectrum was displaced from its preflight position on the detector, indicating that the optic may have shifted within its holder after laboratory calibration. Such a shift could introduce aberrations consistent with the observed resolution loss. We also considered the possibility that the tin filter itself, which is displaced from the focal plane by 2 mm in Z, broadens the effective size of the point source. However, the optical constants indicate that the vast majority of the attenuated light should be absorbed (not scattered), and the extreme thinness of the filter makes it unlikely that the membrane affects the path of the transmitted rays to any appreciable degree.

In Figure 3 we compare the *EUVE* and *ORFEUS-SPAS II* spectra of ϵ CMa in several wavelength regions. The effect of the higher resolution afforded by *ORFEUS-SPAS II* can be clearly seen in this figure, with individual features in the *EUVE* data now resolved into multiple components in the *ORFEUS-SPAS II* data. This increase in resolution will be valuable for testing atmosphere models, which must reproduce the rich spectral features in the EUV as well as the high continuum levels if the mystery of the extraordinary continuum fluxes in very early B giants is to be solved. This figure also shows that the *ORFEUS-SPAS II* EUV spectrometer is indeed about three times more sensitive than the *EUVE* long-wavelength spectrometer. This general result appears to hold over the entire common wavelength range of 520 Å to 665 Å, although the relative sensitivity of *ORFEUS-SPAS II* increases slightly at the long wavelength end of the range.

With the improved resolution of *ORFEUS-SPAS II*, wind features can be resolved, whereas in the *EUVE* spectra of ϵ CMa the presence of wind features could be inferred only from their high ionization stages (Cassinelli et al. 1995). As Figure 4 shows, we can now see the distinctive wind-broadened morphology in the O V line at 630 Å and the S IV doublet at 657, 661 Å. Although other S IV features are seen in ϵ CMa, the resonance lines at 657, 661 Å are the most reliable indicators of wind activity. It should be noted that some features of intermediate ionization stages, such as the O IV lines near 554 Å and 610 Å, are possibly asymmetric and slightly broader than the intrinsically narrow lines used for the spectral resolution determination.

The blue edge velocity of the O V line lies somewhere between 500 and 800 km s^{-1}, depending on the true continuum level and the degree of blending with other features. This range of values is only slightly below the theoretical terminal velocity, and is comparable to the blue edge velocity seen in the C IV 1548, 1551 Å doublet (Snow & Morton 1976).
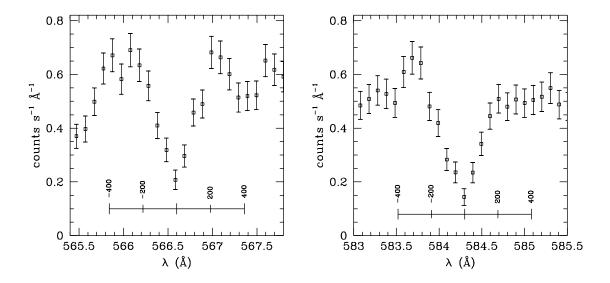
Fig. 2.— Two of the best separated, unblended features in the *ORFEUS-SPAS II* spectrum are shown: Si III on the left and He I on the right. The velocity scale, in km s^{-1}, is indicated at the bottom of each panel. These features are used to determine the effective spectral resolution of the EUV spectrometer.
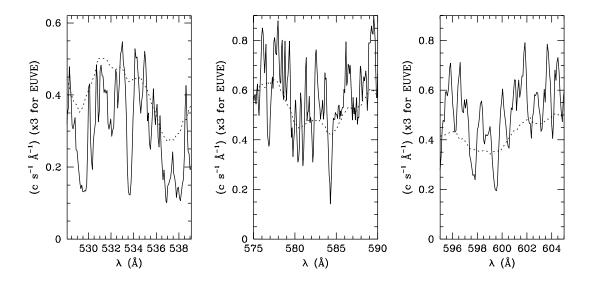

Fig. 3.— We show several portions of the *ORFEUS-SPAS II* spectrum (solid line) with the *EUVE* data (dotted line) for ε CMa overplotted in counts per unit wavelength interval. The *EUVE* spectrum is multiplied by 3 throughout in order to bring its level up to that seen in the *ORFEUS-SPAS II* data.

The S IV lines have blue edge velocities closer to 300 km s^{-1}. This lower velocity may be due to ionization gradients in the winds. By combining these EUV wind lines observed with *ORFEUS-SPAS II*, including the O IV features as well as O V and S IV, with *IUE*, *HST*, *IMAPS*, and *Copernicus* data, it should be possible to place tight constraints on the mass-loss rate, terminal velocity, and ionization balance of the wind of ϵ CMa.

4.   Conclusions

The performance of *ORFEUS-SPAS II* in the EUV was excellent, although the spectral resolution is lower than that generally achieved in the FUV. The effective area, including the tin filter transmission, is about 3 times that of *EUVE*, as expected. The data collected during the flight of the telescope in 1996 pose a strong challenge to the models currently being made to explain the large photospheric flux of ϵ CMa. This is because equivalent widths of individual EUV lines can now be determined. The wind lines, primarily O V, have now been resolved and will provide important new constraints on the wind ionization models of early B stars. Similar EUV spectroscopy of the other known EUV-bright B giant, β CMa, would be very helpful in determining the wind properties and the cause of the high EUV fluxes in early B stars.
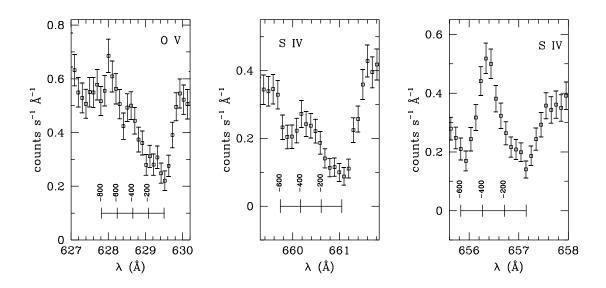

Fig. 4.— Wind broadened oxygen and sulfur lines are shown, with a velocity scale in km s^{-1} indicated at the bottom of each panel. These display the classical asymmetric wind signature, although the mass-loss rate of ϵ CMa is low enough that no P Cygni emission feature is seen. Features that appear near -500 km s^{-1} are due to blends, not the wind.

Acknowledgments

REFERENCES

Aufdenberg, J. P., Hauschildt, P. H., Shore, S. N., & Baron, E. 1998, ApJ, submitted

Cassinelli, J. P. 1996, in *Astrophysics in the Extreme Ultraviolet*, eds. S. Bowyer and R. Malina (Dordrecht: Kluwer), 367

Cassinelli, J. P., Cohen, D. H., MacFarlane, J. J., Drew, J. E., Lynas-Gray, A. E., Hoare, M. G., Vallerga, J. V., Welsh, B. Y., Vedder, P. W., Hubeny, I., & Lanz, T. 1995, ApJ, 438, 932

Cohen, D. H., Cooper, R. G., MacFarlane, J. J., Owocki, S. P., Cassinelli, J. P., & Wang, P. 1996, ApJ, 460, 506

Hubeny, I. & Lanz, T., 1992, A&A, 262, 501

Hurwitz, M. et al. 1997, ApJ, this issue

Hurwitz, M. & Bowyer, S. 1986, Proc. SPIE, 627, 375

Hurwitz, M. & Bowyer, S. 1996, in *Astrophysics in the Extreme Ultraviolet*, eds. S. Bowyer and R. F. Malina (Dordrecht: Kluwer), 601

Kurucz, R.L. 1992, in *Model Atmospheres for Population Synthesis*, eds. B. Barbury, A. Renzini (Dordrecht: Kluwer), 225

Najarro, F., Kudritzki, R. P., Cassinelli, J. P., Stahl, O., & Hillier, D. J. 1996, A&A, 306, 892

Snow, T. P., & Morton, D. C. 1976, ApJS, 32, 429

Uesugi, A., & Fukuda, I. 1982, *Revised Catalog of Stellar Rotational Velocities* (Kyoto: Kyoto University)

Vallerga, J. V., Vedder, P. W., & Welsh, B. Y. 1993, ApJ, 414, L65

Verner, D. A., Verner, E. M., & Ferland, G. J. 1996, Atomic Data Nucl. Data Tables, 64, 1